

Design and Performance Analysis of Rectangular Microstrip Patch Antennas Using Different Feeding Techniques for 5G Applications

Original Scientific Paper

Sattar Othman Hasan

Salahaddin University-Erbil, Iraq
College of Education, Department of Physics
sattar.hasan@su.edu.krd

Saman Khabbat Ezzulddin

Salahaddin University-Erbil, Iraq
College of Science, Department of Physics
saman.ezzulddin@su.edu.krd

Othman Salim Hammd

Salahaddin University-Erbil, Iraq
College of Education, Department of Physics
othman.hammd@su.edu.krd

Rashad Hassan Mahmud

Salahaddin University-Erbil, Iraq
College of Education, Department of Physics
rashad.mahmud@su.edu.krd

Abstract – In this article, the design and performance of a novel rectangular microstrip patch antenna (RMPA) utilizing the dielectric substrate material FR4 of relative permittivity ($\epsilon_r = 4.3$) and thickness ($h = 0.254$ mm) is proposed to operate at ($f_r = 28$ GHz). Three different feeding techniques (microstrip inset line, coaxial probe, and proximity coupled line) are investigated to improve the antenna radiation performance especially the antenna gain and bandwidth using Computer Simulation Technology (CST) and High Frequency Structure Simulator (HFSS). The simulated frequency responses generally reveal that the proximity-coupled fed provides extremely directive pattern and maintain higher radiation performance regardless of its antenna size which is larger than the other considered feeding ones. With the presence of the three feeding techniques, the gain is improved from 5.50 dB to 6.83 dB additionally, the antenna bandwidth is improved from 0.6 GHz to 3.60 GHz at $f_r = 28$ GHz when the reflection coefficient $S_{11} = -10$ dB. Compared to the previously designed RMPA, the proposed design has the advantages of reliable size, larger bandwidth and higher gain, which make it more suitable for many 5G application systems.

Keywords: Feed techniques, gain, broadband bandwidth, microstrip patch, 5G

1. INTRODUCTION

In recent years, wireless applications have been involved in all aspects of our life. Wide bandwidth, high gain, and compactness are the properties of antennas that are extremely required in the 5G and millimeter wave applications [1, 2]. A rectangular microstrip patch antenna (RMPA) is a good candidate to employ in these applications. However, its poor gain and small bandwidth are considered the two main drawbacks. Many methods have been conducted in the literature to overcome these drawbacks.

Numerous studies have been conducted to enhance the gain and bandwidth of MPAs, for instance decreasing substrate thickness, increasing substrate permittivity, feeding methodologies, and using various optimization methods [3]. Moreover, the mode shift theory presented in [4] was mainly done to enhance the bandwidth of the dual-mode RMPA by exciting two resonant modes. Exciting the higher mode in the RMPA has improved the bandwidth and efficiency and reduced the antenna size.

A pair of slots etched from the microstrip patch done in [5] was to excite the two radiative modes close to each other and enlarge the bandwidth of the MPA. On the other hand, a superstrate lens placed on a normal patch antenna, which uniformed the phase distribution of the electric field over the patch was studied by [6] and led to an improvement in the antenna gain up to 48%.

In addition, a ferrite ring realized into the hybrid substrate of the RMPA was proposed by [7] to create a constructive interference between the incident and reflective fields in the substrate, which leads to an enhanced 4.0 dB gain of the antenna without compromising the bandwidth. Subsequently, two sets of short-circuited patches introduced in [8] were to excite two sets of orthogonal electric and magnetic dipole modes and enhance the overall antenna performances. A switchable feed network, which was controlled by a microcontroller, was employed in the array to provide a reconfigurable polarization and a high gain to the RMPA [9]. A numerical method (so-called discrete mode matching method) was presented in [10] to overcome the

disadvantages of RMPA. A microstrip patch was fed optically via a vertical cavity surface emitting laser by [11]. Such an optically feed system removes the need of the transmission line to feed the radiation element to improve the antenna gain.

Different from the methods mentioned above, a dual circularly polarized radiation was obtained from an equilateral triangular patch antenna using an aperture-coupled and proximity feeds [12]. A circular microstrip patch antenna's bandwidth and gain were significantly enhanced using an L-shaped patch with coaxial probe feed and hybrid-feed techniques [13]. Similarly, the dual feed ports in the square microstrip patch antenna were utilized to excite two orthogonal modes [14]. As a result of that, linear and circular polarization can be resulted over a certain operating frequency point. A bow-tie slot, which was etched from a rectangular patch, was introduced to achieve dual polarization and widen the bandwidth of RMPA [15].

This article proposes a new design of RMPA using three feeding techniques: microstrip inset feed, coaxial probe feed, and proximity coupled feed. For this, the dielectric material FR4 is selected as a substrate and the return loss S11, VSWR, gain, radiation pattern, antenna size and bandwidth of the suggested RMPA are examined under the influence of these feeding techniques using the (HFSS) and (CST) simulation methods. Through these investigations, a reasonable feeding technique in terms of simplicity and providing reliable radiation performance suitable for 5G application systems is identified.

The remaining part of the article is arranged as follows. Section 2 presents the theory, calculation, and design of the RMPA in the light of the three feeding techniques. The computed results of the fundamental RMPA parameters with the using each mentioned feeding methods are displayed in section three. Finally, the remarkable outcome conclusions are presented in section four.

2. ANTENNA DESIGN

Generally, different methods existed in the literature to feed the radiation patch of RMPA. The role of which in enhancing the antenna input impedance and efficiency is significant [17]. The two most widely recognized feeding techniques are the contact and non-contact methods. In the case of the contacting method, the guided EM energy is fed immediately to the radiating patch via a conducting strip such as microstrip inset line feeding and/or a coaxial probe feeding. On the other hand, the guided EM energy can be guided to the radiating patch under the resonant condition via proximity coupling fed. In the following, the design of RMPA in the light of these feeding types is described.

2.1. THEORETICAL DESIGN

The three fundamental parameters for the design of RMPA are the resonant frequency (f_r), substrate thickness (h), and substrate relative permittivity (ϵ_r). For

the proposed RMPA, the (f_r) value is chosen to be (28) GHz. The substrate material type is FR4 with dielectric constant ($\epsilon_r = 4.3$) and thickness ($h = 0.254$ mm). The remaining design parameters can be calculated using the following relations.

The patch width (W_p) can be obtained using the relation [18]:

$$W_p = \frac{c}{2f_r} \sqrt{\frac{2}{\epsilon_r + 1}} \quad (1)$$

Where, (c) is the speed of light in free space. The effective relative permittivity (ϵ_{reff}) which is produced due to the creation of fringing field and is expressed for the advanced RMPA as follows [18]:

$$\epsilon_{reff} = \frac{\epsilon_r + 1}{2} + \frac{\epsilon_r - 1}{2} \left[1 + 12 \frac{h}{W_p} \right] \quad (2)$$

The extension patch length (ΔL), which arise due to substrate thickness fringing field effect can be determined by [18]:

$$\Delta L = \frac{0.412(\epsilon_{reff} + 0.3) \left(\frac{W_p}{h} + 0.264 \right)}{(\epsilon_{reff} - 0.258) \left(\frac{W_p}{h} + 0.8 \right)} \epsilon_{eff} \quad (3)$$

And, the effective patch length (L_{eff}) is computed by an expression given by [18] as:

$$L_{eff} = \frac{c}{2f_r \sqrt{\epsilon_{reff}}} \quad (4)$$

Finally, the actual patch length (L_p) can be calculated in term of the L_{eff} and ΔL of the patch using the relation [18]:

$$L_p = L_{eff} - 2\Delta L \quad (5)$$

It is worth mentioning that the above relations have been utilized to obtain the initial physical dimensions of the proposed RMPA. These dimensions have been inserted into the CST and HFSS simulators so as to layout the actual RMPA as can be seen in the next section.

2.2. ANTENNA CONFIGURATION

Fig. 1 demonstrates the design of the recommended RMPA with the presence of the three feeding techniques using the (CST) simulator. Fig. 1 (a), represents the RMPA which is fed via the microstrip inset feed line. Such line is used to convert the edge impedance to a merit that matches to the input impedance characteristic. Two slots are etched around the microstrip line in order to maintain good impedance matching. The length of the microstrip feed line is a quarter wavelength within the transformed impedance value that can be computed using the relation [19]:

$$Z_T = \sqrt{Z_o Z_a} \quad (6)$$

Here, Z_o is the applied source impedance, Z_a is the radiation patch input impedance, and Z_T is impedance of the microstrip feed line.

In Fig. 1 (b), the design of the proposed RMPA with the existence of the proximity-coupled feed is shown. In this case, the antenna compasses the two layers of

dielectric medium with the same substrate thickness and dielectric constant. In Fig. 1 (c), the radiation patch is powered by a coaxial feed technique. This technique requires a probe feed line (mainly a 50 Ω coaxial connector) to link the radiation patch to the input port. The edge position of the port can be computed using the expression given by [17] as:

$$y(y_o) = \cos^2\left(\frac{\pi y_o}{L}\right) \quad (7)$$

Where, (y_o) is the y-position of the fed point at which the impedance matching is occur.

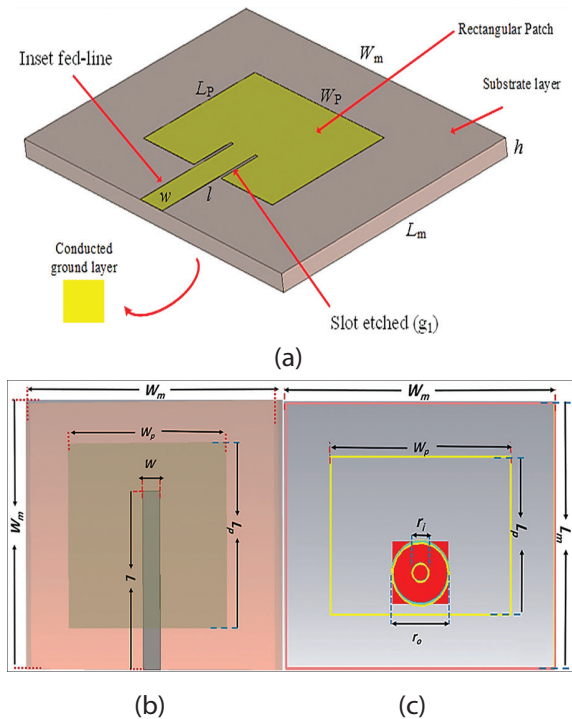


Fig. 1. Three-dimensional view of the simulated RMPA with their specified layer representation for (a) microstrip line, (b) Proximity coupled and (c) Coaxial probe fed

It is essential to observe that the initial values of the dimensions labeled on the RMPA in Fig. 1 have been obtained using the relations given in section 2.1. Then, the genetic algorithm optimization method in CST has been performed on these dimensions in order to make the antenna resonate at ($f_r = 28$ GHz). The optimized dimensions of the proposed RMPA with each mentioned feeding techniques are summarized in Table 1.

Table 1. Optimized physical dimensions of the proposed RMPAs with each feeding techniques

Parameters (mm)	Discription	Feed Types		
		Microstrip line	Coaxial probe	Proximity coupled
W_p	Patch Width	3.92	4.41	4.13
L_p	Patch Length	2.42	3.54	4.0

W_m	Width of ground Plane	6.58	6.58	6.58
L_m	Length of ground Plane	5.79	5.79	5.79
g_1	Slot etched	0.08	--	--
L	Length of Feed Line	0.88	--	3.86
h	Substrate Hight	0.254	0.254	0.508
W	Feed line with	0.49	--	0.44
r_o	Outer conductor diameters	--	1.40	--
r_i	Inner conductor diameter	--	0.40	--

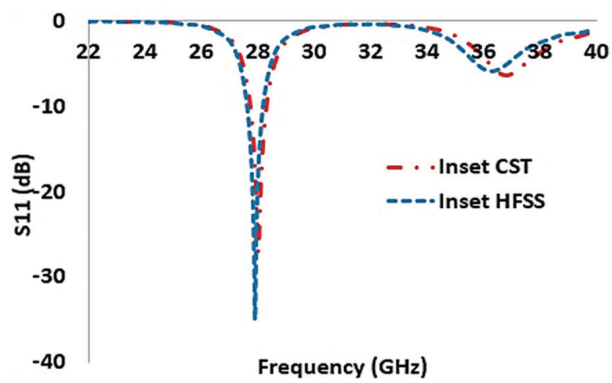
3. RESULTS AND DISCUSSIONS

This section exhibits the proposed RMPA simulation results with the mentioned feeding technique using the CST and HFSS simulators. It can be indicated that good agreement between the simulated results of the CST and HFSS are obtained, validating the accuracy of the suggested RMPAs.

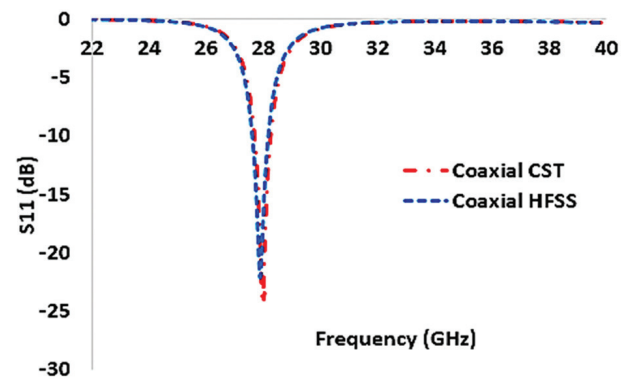
Fig. 2 represents the simulated results of the advanced RMPA feeding with the microstrip inset feed line. As can be observed form Fig. 2 (a) that the reflection coefficient (S_{11}) is well matched at $f_r = 28$ GHz having about 0.60 GHz bandwidth at ($S_{11} = 10$ dB). The first peak gain value is 5.50 dB at (28) GHz, while, the second peak gains value is 4.61 dB appeared at (37) GHz, as can be noticed in Fig. 2 (b). The radiation pattern for both the electric (E) and magnetic (H) planes are shown in Fig. 2 (c) and (d) at which the main beam is extremely directive with having small back lobes.

Moreover, the computed results obtained with both HFSS and CST simulation techniques of the recommended RMPA, when the coaxial feed probe feed is employed are displayed in Fig. 3. A very good matching of S_{11} is achieved at (28) GHz as shown in Fig. 3 (a). Also, about 0.6 GHz bandwidth is obtained at frequency of (28) GHz when ($S_{11} = -10$ dB). The maximum gain is 6.73 dB at (27) GHz as can be noticed in Fig. 3 (b). Moreover, the antenna radiation patterns are very directive for both the E- and H-planes at (28) GHz having only one back lobe as clearly seen in Fig. 3 (c) and (d). The existence of the back lobe here is appear due to the coaxial probe feed located beneath the RMPA which could distort the electric field distribution.

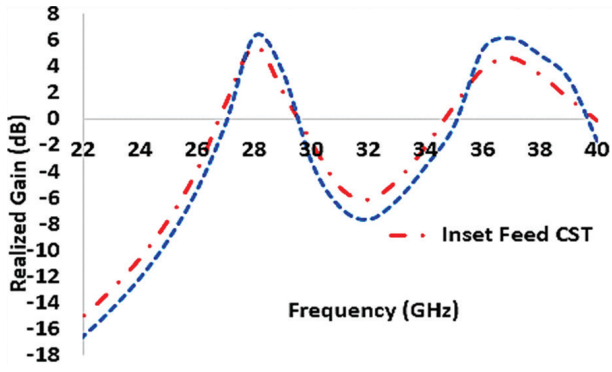
The proposed RMPA, when the proximity coupled probe is employed, is also simulated in both the CST and HFSS simulators. The calculated results are presented in Fig. 4. It can be observed from Fig. 4 (a) that the proposed RMPA provides a very large bandwidth, which is more than 3.60 GHz at $f_r = 28$ GHz with the implementation of proximity coupled fed.



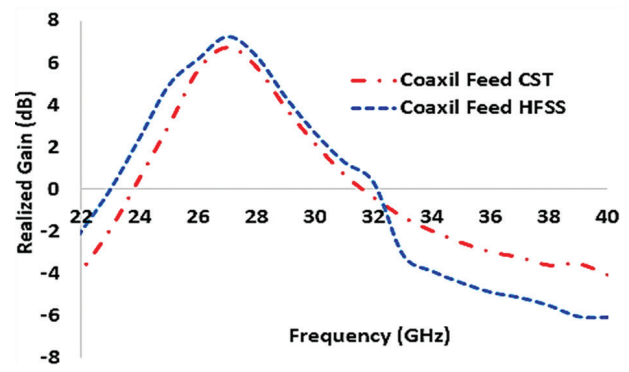
(a)



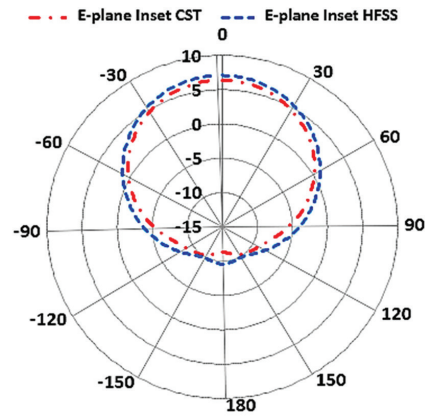
(a)



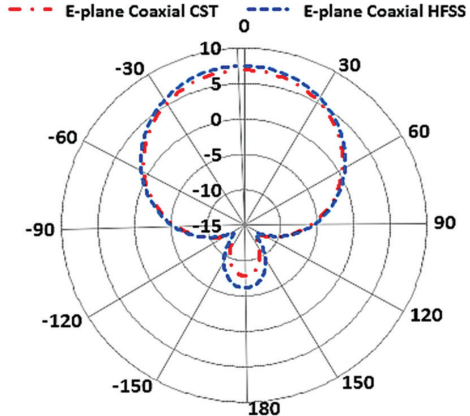
(b)



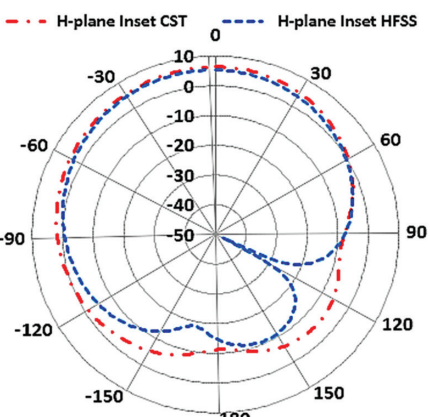
(b)



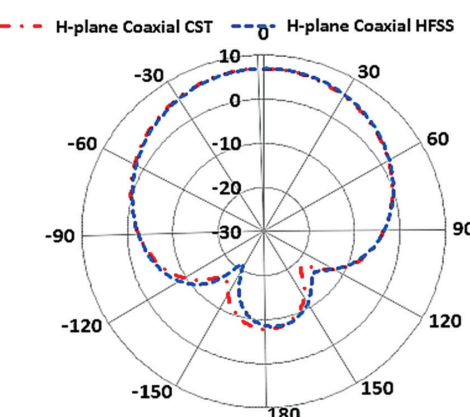
(c)



(c)



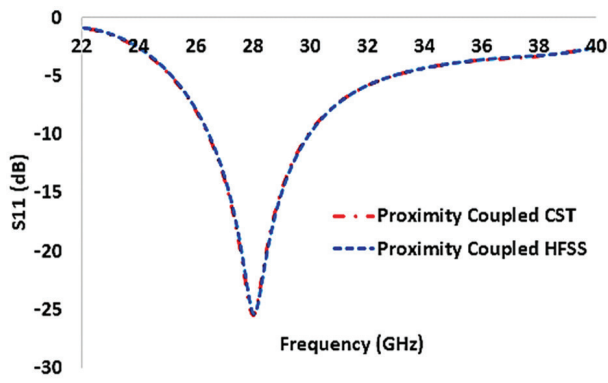
(d)



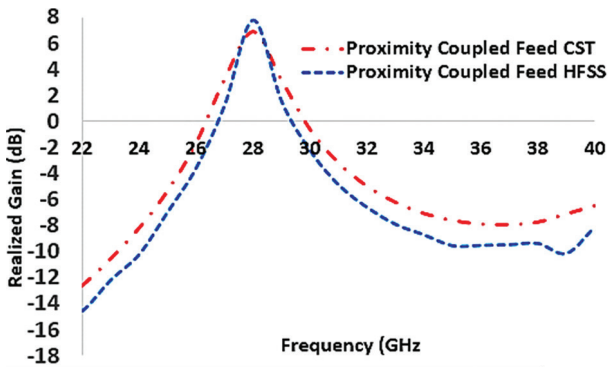
(d)

Fig. 2. Demonstrates results of the (a) Reflection coefficient (S11), (b) Realized gain, (c) E-plane and (d) H-plane for RMPA with the microstrip inset feed line

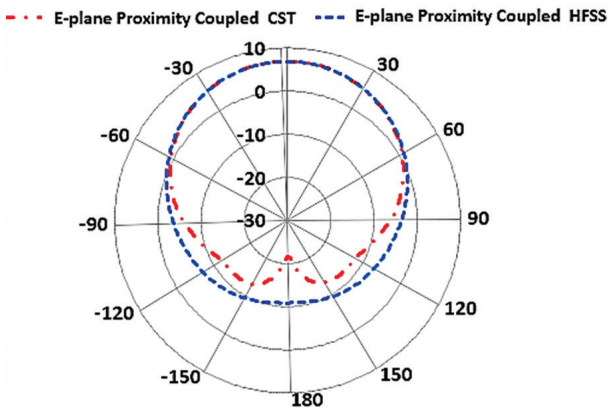
Fig. 3. Represents results of the (a) Reflection coefficient (S11), (b) Realized gain, (c) E-plane and (d) H-plane for RMPA with the coaxial probe feed



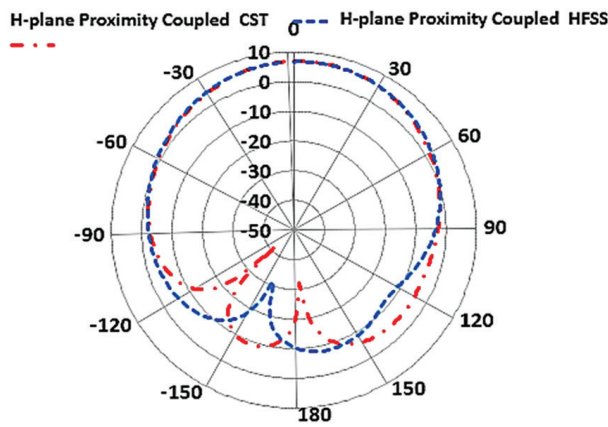
(a)



(b)



(c)

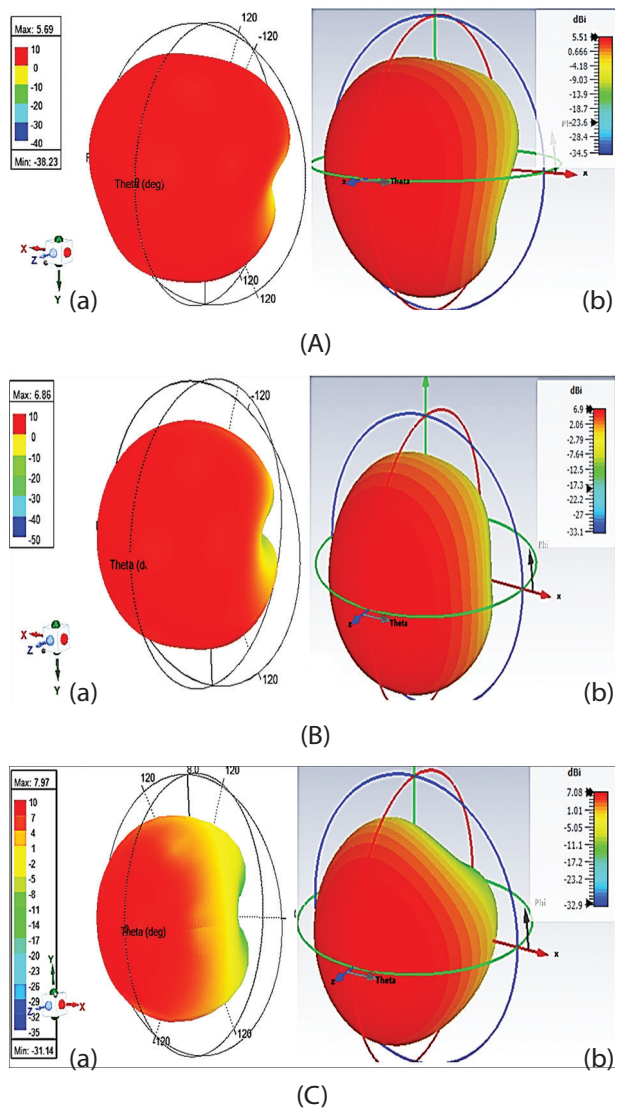


(d)

Fig. 4. displays results of the (a) Reflection coefficient (S11), (b) Realized gain, (c) E-plane and (d) H-plane for RMPA with the proximity coupled feed

Also, Fig. 4 (b) indicates that the peak gain value is 6.86 dB at $f_r = 28$ GHz. Besides, extremely directive E- and H-planes radiation pattern with low side lobe level are observed with the proximity coupled fed as shown in Fig. 4 (c) and (d).

In addition, both CST and HFSS simulators are employed to compute the antenna directivity. The results of these computation for each considered feeding technique are shown in 3D view in Fig. 5. The HFSS simulator results reveal that the directivity values are (5.690, 6.860 and 7.980) dB for inset, coaxial and proximity-coupled feed, respectively for RMPA operating at (28) GHz. Additionally, the directivity values achieved for microstrip inset line, coaxial probe and proximity coupled feed with the implementation of CST simulator, are (5.515, 6.905 and 7.075) dB, respectively.

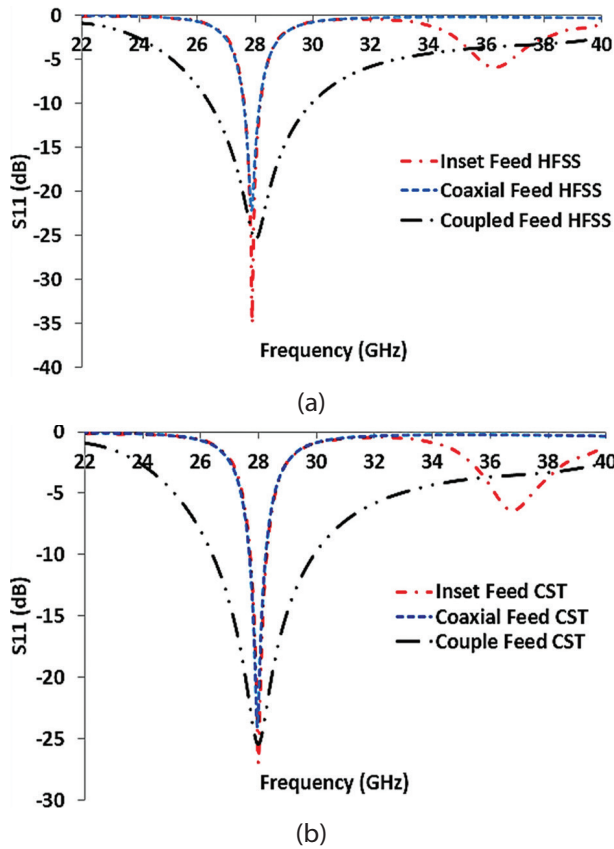


Figs. 5. 3D view of RMPA directivity obtained by (a) HFSS and (b) CST for (A) microstrip inset fed, (B) coaxial probe fed and (C) proximity coupled fed.

The achieved values from both modeling techniques well agree with each other and the best values of antenna directivity are recorded with the proximity-cou-

pled feed technique, while it can be seen that directivity for both the inset and coaxial feeding methods are nearly equal [17].

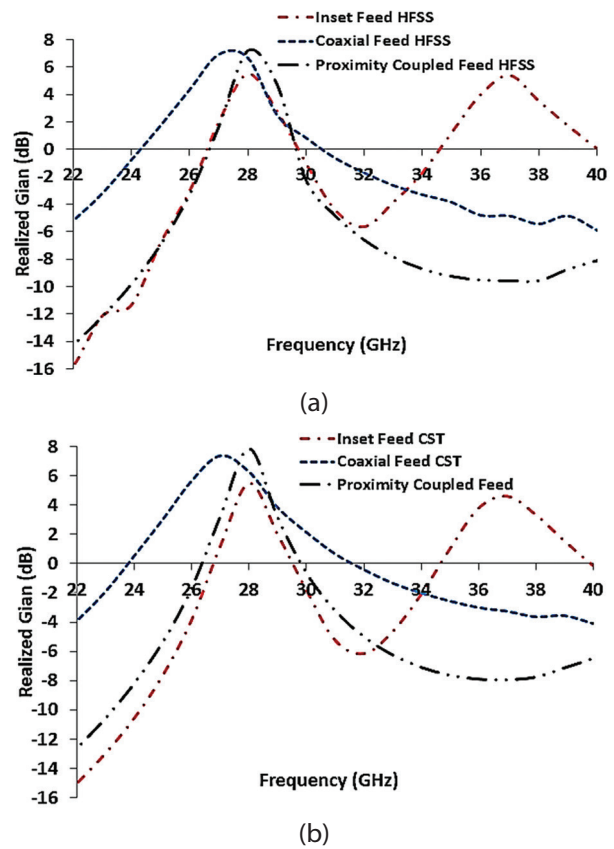
On the other hand, the calculated bandwidth obtained with both simulation methods and for each aforementioned feeding techniques reveal that the



Figs. 6. The simulated antenna returns loss of the proposed RMPA with the presence of aforementioned feeding techniques with the use of (a) HFSS and (b) CST

Finally, the overall calculated RMPA parameters obtained with both HFSS and CST simulation methods are summarized in Table 2 and compared with previous investigation by other researchers using different feeding methods. Table 2 exhibits the advantages of the

proximity coupled feed technique has enlarged the bandwidth from 0.6 GHz to 3.60 GHz when $S_{11} = -10$ dB at $f_r = 28$ GHz as represented in Fig. 6. Besides, the maximum value of realized gain is equal to 6.86 dB, which is achieved with using proximity coupled technique as observed in Fig. 7.



Figs. 7. The simulated antenna realized gain of the proposed RMPA with the presence of aforementioned feeding techniques with the use of (a) HFSS and (b) CST.

proposed design, when the proximity coupled probe is employed, over the previously designed RMPA in the literature. It can be seen that our design is very competitive to the cited works, particularly in terms of the total size and overall radiation performances.

Table 2. Overall calculated RMPA parameters obtained with both HFSS and CST simulation methods

Simulation method	S11 (dB)	VSWR	Gain (dB)	BW(GHz)	fr(GHz)	Size mm3	Reference
Inset HFSS	-14.00	1.499	1.890	0.540	28.00	-	[20]
Inset HFSS	-40.08	1.020	4.060	-	27.50	324.958	[21]
Inset HFSS	-22.20	1.340	6.850	-	28.00	22.365	[22]
Inset HFSS	-24.50	1.127	6.430	0.900	27.65	23.400	[23]
Inset HFSS	-20.64	1.20	6.290	0.369	28.00	-	[24]
Inset HFSS	-20.00	1.222	8.020	1.300	28.00	22.702	[25]
Inset HFSS	-32.86	1.047	3.590	1.450	28.00	-	[26]
Inset HFSS	-35.03	1.028	6.690	0.595	27.98	9.676	Present work
Inset CST	-12.59	1.613	6.690	0.582	27.91	29.517	[27]
Inset CST	-20.53	1.020	6.210	0.400	27.98	119.07	[28]

Inset CST	-14.15	1.488	6.060	0.800	28.00	185.80	[29]
Inset CST	-36.17	1.310	6.710	0.462	27.98	19.124	[30]
Inset CST	-22.50	1.162	7.200	1.610	26.00	59.695	[31]
Inset CST	-28.68	1.076	5.820	0.452	28.00	-	[24]
Inset CST	-67.37	1.001	7.750	0.660	28.20	-	[32]
Inset CST	-26.00	1.160	4.430	2.900	28.02	17.050	[33]
Inset CST	-38.34	1.024	8.200	3.464	28.08	244.619	[34]
Inset CST	-20.09	1.197	7.500	1.060	28.00	46.350	[35]
Inset CST	-27.04	1.095	5.515	0.573	28.00	9.676	Present work
Coaxial HFSS	-27.00	1.094	7.800	1.700	27.23	23.400	[23]
Coaxial HFSS	-21.95	1.170	7.110	0.259	28.00	-	[24]
Coaxial HFSS	-20.00	1.222	6.510	2.200	28.10	22.702	[25]
Coaxial HFSS	-36.60	1.030	4.170	0.800	28.00	-	[26]
Coaxial HFSS	-24.72	1.123	6.860	0.557	27.94	9.676	Present work
Coaxial CST	-24.00	1.135	7.500	2.610	26.00	59.695	[31]
Coaxial CST	-43.23	1.014	7.690	0.792	28.30	-	[32]
Coaxial CST	-21.26	1.180	6.050	0.356	28.00	-	[24]
Coaxial CST	-24.02	1.134	6.904	0.589	27.98	9.676	Present work
Proximity HFSS	-25.44	1.112	7.075	3.616	28.00	19.350	Present work
Proximity CST	-28.39	1.113	7.980	3.586	27.46	19.350	Present work

4. CONCLUSIONS

In this work, a new configuration of RMPA operating at 28 GHz has been proposed using three different feeding techniques: the microstrip inset, the coaxial probe, and the proximity coupled. The characteristics of the simulated RMPA have been determined using the HFSS and CST simulators. Although the proximity coupled feed is some complex in terms of manufacturing, but generally gives higher radiation performance compared to the other considered feeding techniques. Since, the simulated results of the proximity coupled fed reveal that the RMPA can provide a gain and bandwidth of the order of (6.86 dB and 3.60 GHz), respectively, with no side and back lobes compared to the other considered feeding techniques. Besides, the proposed design has a very small size and competitive gain and bandwidth when compared to the other works cited here. In addition, it should be observed that the presented RMSAs are acceptable for use in 5G wireless communication systems.

5. REFERENCES

- [1] B. A. Rahman, S. O. Hasan, "Simulation Design of Low-Profile Equilateral Triangle Microstrip Patch Antenna Operating at 28 GHz", *International Journal on Communications Antenna and Propagation*, Vol. 12, 2022, pp. 74-82.
- [2] D. H. Patel, G. D. Makwana, "A Comprehensive Review on Multi-band Microstrip Patch Antenna Comprising 5G Wireless Communication", *International Journal of Computing and Digital System*, Vol. 11, 2022, pp. 942-953.
- [3] A. Bansal, R. Gupta, "A review on microstrip patch antenna and feeding techniques", *International Journal of Information Technology*, Vol. 12, 2020, pp. 149-154.
- [4] A. Bhattacharyya, J. Pal, K. Patra, B. Gupta, "Bandwidth-enhanced miniaturized patch antenna operating at higher order dual-mode resonance using modal analysis", *IEEE Antennas and Wireless Propagation Letters*, Vol. 20, 2020, pp. 274-278.
- [5] J. Wen, D. Xie, L. Zhu, "Bandwidth-Enhanced High-Gain Microstrip Patch Antenna Under TM Dual-Mode Resonances", *IEEE Antennas and Wireless Propagation Letters*, Vol. 18, 2019, pp. 1976-1980.
- [6] M. S. M. Mollaei, E. Zanganeh, M. F. Farahani, "Enhancement of patch antenna gain using cylindrical shell-shaped superstrate", *IEEE Antennas and Wireless Propagation Letters*, Vol. 16, 2017, pp. 2570-2573.
- [7] A. Rivera-Albino, C. A. Balanis, "Gain enhancement in microstrip patch antennas using hybrid substrates", *IEEE Antennas and Wireless Propagation Letters*, Vol. 12, 2013, pp. 476-479.
- [8] Y. Liu, Z. Yue, Y. Jia, Y. Xu, Q. Xue, "Dual-band dual-circularly polarized antenna array with printed

- ridge gap waveguide", *IEEE Transactions on Antennas and Propagation*, Vol. 69, 2021, pp. 5118-5123.
- [9] C. Liu, Y. Li, T. Liu, Y. Han, J. Wang, S. Qu, "Polarization reconfigurable and beam-switchable array antenna using switchable feed network", *IEEE Access*, Vol. 10, 2022, pp. 29032-29039.
- [10] A. Ioffe, M. Thiel, A. Dreher, "Analysis of microstrip patch antennas on arbitrarily shaped multilayers", *IEEE Transactions on Antennas and Propagation*, Vol. 51, 2003, pp. 1929-1935.
- [11] F. Peressutti, B. Poussot, L. Rousseau, C. Viana, J.-M. Laheurte, J.-L. Polleux, "Optically-Fed 5GHz Patch Antennas Excited by Vertical-Cavity Surface-Emitting Lasers", *Journal of Lightwave Technology*, Vol. 39, 2021, pp. 6768-6773.
- [12] Q. Luo, S. Gao, M. Sobhy, J. T. S. Sumantyo, J. Li, G. Wei, J. Xu, C. Wu, "Dual circularly polarized equilateral triangular patch array", *IEEE Transactions on Antennas and Propagation*, Vol. 64, 2016, pp. 2255-2262.
- [13] S.-L. Yang, K.-M. Luk, "Design of a wide-band L-probe patch antenna for pattern reconfiguration or diversity applications", *IEEE Transactions on Antennas and Propagation*, Vol. 54, 2006, pp. 433-438.
- [14] J.-F. Tsai, J.-S. Row, "Reconfigurable square-ring microstrip antenna", *IEEE Transactions on Antennas and Propagation*, Vol. 61, 2013, pp. 2857-2860.
- [15] C. Deng, Y. Li, Z. Zhang, Z. Feng, "A wideband high-isolated dual-polarized patch antenna using two different balun feedings", *IEEE Antennas and Wireless Propagation Letters*, Vol. 13, 2014, pp. 1617-1619.
- [16] S. K. Ezzulddin, S. O. Hasan, M. M. Ameen, "Microstrip patch antenna design, simulation and fabrication for 5G applications", *Simulation Modelling Practice and Theory*, Vol. 116, 2022, p. 102497.
- [17] P. Kuravatti, "Comparison of different parameters of the edge feed and the inset feed patch antenna", *International Journal of Applied Engineering Research*, Vol. 13, 2018, pp. 11285-11288.
- [18] Y. Huang, "Antennas: from theory to practice", John Wiley & Sons, 2021.
- [19] C. A. Balanis, "Antenna Theory Analysis and Design", 4th Edition, John Wiley & Sons, 2016.
- [20] Y. S. Khraisat, "Increasing microstrip patch antenna bandwidth by inserting ground slots", *Journal of Electromagnetic Analysis and Applications*, Vol. 10, 2018, pp. 1-11.
- [21] K. Neha, S. Sunil, "A 28-GHz U-slot microstrip patch antenna for 5G applications", *International Journal of Engineering Development and Research*, Vol. 6, 2018, pp. 363-368.
- [22] A. Sivabalan, S. Pavithra, R. Selvarani, K. Vinitha, "Design of microstrip patch antenna for 5G", *International Journal of Control and Automation*, Vol. 13, 2021, pp. 546-552.
- [23] I. Gharbi, R. Barrak, M. Menif, H. Ragad, "Design of patch array antennas for future 5G applications", *Proceedings of the 18th International Conference on Sciences and Techniques of Automatic Control and Computer Engineering*, Monastir, Tunisia, 21-23 December 2017, pp. 674-678.
- [24] B. A. Rahman, S. O. Hasan, "Radiation Performance of Different Triangular Microstrip Patch Antenna Configuration Shapes Operating at 28 GHz", *Zanco Journal of Pure and Applied Sciences*, Vol. 34, 2022, pp. 45-55.
- [25] P. Yugandhar, P. M. Rao, "Design And Performance Analysis of Single Patch Antenna, Slotted Patch Antenna And 1x2 Antenna Array For 5G Applications", *International Research Journal of Modernization in Engineering Technology and Science*, Vol. 4, 2022, pp. 1272-1279.
- [26] K. Lalitha, K. L. Bhavani, P. Siddaiah, "Performance Analysis of Hybrid Microstrip Patch Antenna at Ka-Band", *International Journal of Advanced Research in Computer and Communication Engineering*, Vol. 5, 2016, pp. 161-165.
- [27] D. Mungur, S. Duraikannan, "Microstrip patch antenna at 28 GHz for 5G applications", *Journal of Science Technology Engineering and Management-Advanced Research & Innovation*, Vol. 1, 2018, pp. 20-22.
- [28] S. Johari, M. A. Jalil, S. I. Ibrahim, M. N. Mohammad, N. Hassan, "28 GHz microstrip patch antennas for future 5G", *Journal of Engineering and Science Research*, Vol. 2, 2018.
- [29] M. Kavitha, T. D. Kumar, A. Gayathri, V. Koushick, "28GHz printed antenna for 5G communication

with improved gain using array", *International Journal of Scientific and Technology Research*, Vol. 9, 2020, pp. 5127-5133.

- [30] M. Darsono, A. Wijaya, "Design and simulation of a rectangular patch microstrip antenna for the frequency of 28 GHz in 5G technology", *Journal of Physics: Conference Series*, Vol. 1469, 2020, pp. 1-7.
- [31] H. Ai, C. Wu, S. Zhou, "Design and simulation of rectangular microstrip patch antenna with 5Gmm-wave coaxial line back-feed and microstrip line side-feeds", *Proceedings of the 5th International Conference on Information Science, Computer Technology and Transportation*, Shenyang, China, 13-15 November 2020, pp. 179-182.
- [32] S. Kumar, A. Kumar, "Design of circular patch antennas for 5G applications", *Proceedings of the 2nd International Conference on Innovations in Electronics, Signal Processing and Communication*, Shillong, India, 1-2 March 2019, pp. 287-289.
- [33] A. A. Ibrahim, H. Zahra, O. M. Dardeer, N. Hussain, S. M. Abbas, M. A. Abdelghany, "Slotted Antenna Array with Enhanced Radiation Characteristics for 5G 28 GHz Communications", *Electronics*, Vol. 11, 2022, pp. 1-13.
- [34] M. S. Rana, M. M. R. Smieeee, "Design and analysis of microstrip patch antenna for 5G wireless communication systems", *Bulletin of Electrical Engineering and Informatics*, Vol. 11, 2022, pp. 3329-3337.
- [35] S.-E. Didi, I. Halkhams, M. Fattah, Y. Balboul, S. Mazer, M. El Bekkali, "Design of a microstrip antenna patch with a rectangular slot for 5G applications operating at 28 GHz", *TELKOMNIKA (Telecommunication Computing Electronics and Control)*, Vol. 20, 2022, pp. 527-536.